Classifying the Asymptotic Behaviors of Semidiscrete Curve-Shortening Flows

Mitchell Eithun

Abstract

A semidiscrete curve-shortening flow continuously deforms a polygon in the direction of an inward normal until it shrinks to a point. We are interested in the long-time behavior of polygons under such flows. Is there a semidiscrete flow under which all polygons become asymptotically regular? This is an open question, but we provide numerical evidence to suggest that the recent β-polygon flow of Glickenstein and Liang produces regular polygons. It is known that triangles become regular under the β-polygon flow. Using a rescaled flow in which a regular polygon is a fixed point, we note how side lengths and angles evolve under the β-polygon flow and conjecture that all quadrilaterals become rhombic and polygons with more than 5 vertices become regular.

1 Introduction

In differential geometry, the *curve-shortening flow* is a geometric flow that continuously deforms simple, closed curves in $\mathbb{R}^2$ by pushing in the direction of an inner-normal vector. The Gage-Hamilton-Grayson Theorem says that in finite time the curve-shortening flow shrinks closed plane curves to round points. In other words, curves asymptotically look like circles under the curve-shortening flow, demonstrated in Figure 1.

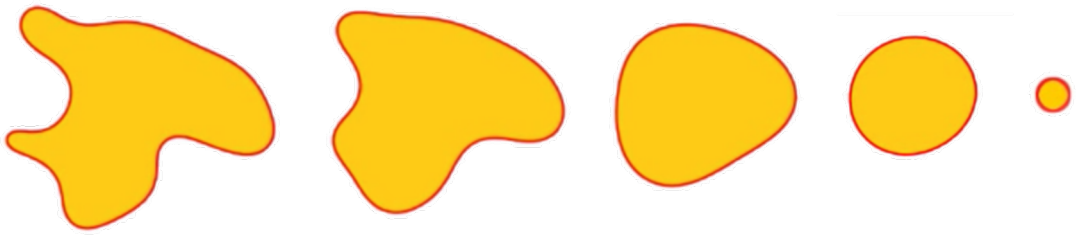

Figure 1: The curve-shortening flow shrinks plane curves to round points [1].

Analogously, *semidiscrete curve-shortening flows* evolve polygons along an inner-normal vector. There is no well-defined inner-normal for polygons and so different semidiscrete curve-shortening schemes rely on different notions of a "normal" direction.

Figure 2: The evolution of a triangle under a semidiscrete curve-shortening flow.

The simplest semidiscrete curve-shortening flow is the one considered by Chow and Glickenstein, in which the evolution is defined by a linear system of differential equations [2]. Under this flow, a polygon asymptotically becomes the affine transformation of a regular polygon, but not necessarily a regular polygon. Since the continuous curve-shortening flow makes plane curves circular, we would like a semidiscrete flow that deforms polygons into regular polygons, which are discrete approximations of the circle. Such a flow has not yet been identified.

One candidate for a flow that produces regular polygons is the β-polygon flow introduced by Glickenstein and Liang [3]. The authors prove that, under the flow, all triangles become regular and polygons with more than 5 vertices are asymptotically stable, meaning that there exists some neighborhood of polygons around each regular polygon that all become asymptotically regular.

To study long-term effects of a geometric flow, it is useful to identify *self-similar solutions*, which simply rescale themselves under a flow. Often self-similar solutions will be asymptotically stable and a flow can be rescaled so that self-similar solutions are fixed points. In the continuous case, the simplest example of a self-similar solution is a circle, which remains circular throughout the flow. In the semidiscrete setting, self-similar solutions are polygons that simply rescale themselves throughout the flow. Notably, all regular polygons are self-similar solutions under the β-polygon flow.

In an effort to strengthen current results about the long-term behavior of the β-polygon flow, we numerically estimate the trajectories of several polygons under the flow. Using a rescaled flow in which a regular polygon is a fixed point, we apply Euler's Method to approximate the trajectories of different size polygons during the evolution process. In the case of the triangle, our results illustrate the fact that all triangles become regular under the flow. For polygons with 5 or more vertices, our evidence suggests that the flow produces regular polygons. In the case of 4 vertices, we suspect that the flow produces rhombuses. In other words, quadrilaterals become equilateral but not necessarily equiangular under the flow.

1.1 Outline

This paper is laid out as follows. In Section 2 we provide a brief overview of the continuous curve-shortening flow to motivate our discussion of semidiscrete flows. In Section 3 we define a polygon and discuss semidiscrete flows on polygons. In Section 4 we discuss the linear semidiscrete flow of Chow and Glickenstein [2]. In Section 5 we discuss the β-polygon flow developed by Glickenstein and Liang [3], a generalization of the linear semidiscrete flow. In

Section 6 we numerically compute the trajectories of different polygons under the β-polygon flow. In Section 7 we discuss the utility of our numerical results and ideas for future work.

2 Continuous Curve-Shortening

To motivate semidiscrete curve-shortening schemes on polygons we start with a brief overview of the continuous curve-shortening flow, which deforms plane curves.

Consider the parametrized curve $X(u) : S_1 \to \mathbb{R}^2$. The curve X is known as a *plane curve* since it is an embedding of a circle into the plane. We think of the plane curve X as being traced out over time with time parameter u. If a plane curve encloses finite area, it is called *closed* and if it does not have self-intersections it is called *simple*. A simple, closed plane curve is *convex* if it encloses a convex region of the plane.

At a point on a simple, closed plane curve, the *unit inner-normal vector* is the unit vector perpendicular to the tangent vector that points into the interior of the curve. The *signed curvature* at a point is a scalar that locally describes how the curve bends, with sign determined by local concavity. (For precise derivations of these quantities, see [4].) The curve-shortening flow deforms simple, closed plane curves at every point in the direction of the unit inner-normal vector scaled by signed curvature, illustrated in Figure 3.

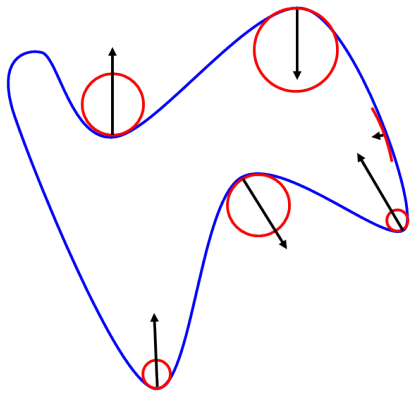

Figure 3: The direction of the deformation made by the curve-shortening flow at a point on a curve is the unit inner-normal vector scaled by signed curvature. Curvature can be thought of as the inverse of the radius of the *osculating circle*, which locally approximates the shape of the curve.

From [5], we have the following definition of the curve-shortening flow.

Definition 1. *Let $X = \{X_t \mid t \in [0, A)\}$ be a family of simple, closed curves, where $X_t(u) : S_1 \to \mathbb{R}^2$. We say X is a solution to the curve-shortening flow if*

$$\frac{\partial X}{\partial t} = \kappa N, \tag{1}$$

where κ is signed curvature and N is the unit inner-normal vector.

2.1 Long-Time Behavior

The long-time behavior of the cure-shortening flow (what happens to a curve as the flow is applied) has been understood since the 1980s. Gage and Hamilton showed that a simple, closed, convex curve converges to a round point under the curve-shortening flow, meaning there is a time that when the curve is as circular as we like before it vanishes [6]. In other words, the curve becomes asymptotically circular under the flow.

Theorem 2.1 (Gage and Hamilton, 1986)**.** *If $X_t(u)$ is a solution to the curve-shortening flow with $X_0(u)$ a convex, closed, embedded curve in $\mathbb{R}^2$, then there exists a $T > 0$ such that the flow exists for all $t \in [0, T)$, $X_t(\cdot)$ is convex for all $t \in [0, T)$, and $X_t(\cdot)$ converges to a round point as $t \to T^-$.*

Grayson later showed that any closed plane curve becomes convex under the curve-shortening flow [7].

Theorem 2.2 (Grayson, 1987)**.** *If $X_t(u)$ is a solution to the curve-shortening flow with $X_0(u)$ a curve embedded in $\mathbb{R}^2$, then there exists a $T > 0$ such that the flow exists in $[0, T]$ and $X_T(u)$ is convex.*

Together Theorems 2.1 and 2.2 establish that all simple, closed plane curves become asymptotically circular under the curve-shortening flow. (This is illustrated in Figure 1.) This result is called the Gage-Hamilton-Grayson Theorem. Analogous results hold for flows on curves in higher dimensional Euclidean space [8].

2.2 Self-Similar Solutions

A *self-similar* solution to the curve-shortening flow is a curve that is rescaled during the flow.

Definition 2. *Let $X = \{X_t \mid t \in [0, A)\}$ be a solution to (1). We say X_0 is self-similar solution of (1) if there exists a scaling function $\lambda(t)$ such that $X_t = \lambda(t)X_0$ for all $t \in [0, A)$.*

All self-similar solutions to the continuous curve-shortening flow have been fully-classified [9]. The circle is the simplest example.

Example 1. Consider a collection of curves $X = \{X_t(\theta) \mid t \in [0, A)\}$, where $X_t(\theta) = r(t)(\cos(\theta), \sin(\theta))$. For each t, the curve $X_t(\theta)$ has curvature $\kappa = \frac{1}{r(t)}$ and unit normal vector $N = (-\cos(\theta), -\sin(\theta))$.

Taking X to be a solution to the curve-shortening flow (1),

$$r'(t)(\cos(\theta),\ \sin(\theta)) = \frac{1}{r(t)}(-\cos(\theta),\ -\sin(\theta)).$$

Hence, $r'(t) = \frac{-1}{r(t)}$ and so $r(t) = \sqrt{-2t + r(0)^2}$. Under the curve-shortening flow, the curve $X_0(\theta)$ shrinks to a circular point. If we set $r = 0$ we find that the curve becomes a point at time $t = \frac{1}{2}r(0)^2$. One interpretation of this result is that if a solution to curve-shortening flow is a circle at some time during the flow, then it is always a circle under the flow.

In general, self-similar solutions of a geometric flow are useful because they can be made fixed-points of a flow to create *rescaled flows* in which curves do not vanish. This makes it easier to study the asymptotic behavior of curves under a particular flow.

2.3 Extensions

Extensions of the curve-shortening flow include *mean curvature flow*, which deforms curves in the more general context of Riemannian manifolds, and *Ricci flow*, which evolves metrics on surfaces [5]. Applications of the curve-shortening flow include isoparametric inequalities [10], robotics [11] and computer vision [12].

Curve-shortening theory for plane curves has been developed over several decades, but as we will see in the next section, fully-analogous results for evolving polygons have not yet been established.

3 Polygons and Curve-Shortening

The focus of this paper is on discrete analogues of the curve-shortening flow that continuously evolve polygons. We call such processes *semidiscrete curve-shortening flows* since they apply a continuous flow to discrete polygons. There also exist *fully-discrete* curve-shortening schemes which use an updating rule rather than a differential equation to evolve polygons [13].

3.1 Polygons

First we define what we mean by a polygon.

Definition 3. *Let $n \geq 3$ and $p \geq 2$. A polygon (or n-gon) X is a collection of vertices $X = \{X_0, X_1, \ldots, X_{n-1}\}$ in $\mathbb{R}^p$.*

Although a polygon is a collection of points we will also consider the line segments $\overline{X_0X_1}$, $\overline{X_1X_2}$, $\ldots$, $\overline{X_{n-2}X_{n-1}}$, $\overline{X_{n-1}X_0}$ to be the *edges* of a polygon. Note that our definition allows edges to intersect at points that are not vertices, like in the heptagon in Figure 4. However, every 3-gon is a triangle in the usual sense.

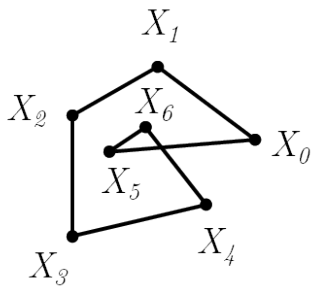

Figure 4: A heptagon in $\mathbb{R}^2$ with interesting edges.

In the $p = 2$ case, we can identify a polygon in $\mathbb{R}^2$ with a vector in $\mathbb{C}^n$, writing

$$X = \begin{pmatrix} X_0 \\ X_1 \\ \vdots \\ X_{n-1} \end{pmatrix} = \begin{pmatrix} x_0 + y_0 i \\ x_1 + y_1 i \\ \vdots \\ x_{n-1} + y_{n-1} i \end{pmatrix}.$$

This allows us to think of each vertex of a polygon as a point in $\mathbb{R}^2$ or as one imaginary number.

3.2 Polygon Flows

As with the continuous flow, we are interested in describing the long-term behavior of semidiscrete flows and the shapes of self-similar solutions. In the continuous case, the curve-shortening flow shrinks all simple, closed plane curves to round points. However, the following important question about polygon evolution is still open.

Question 3.1. *Is there a semidiscrete curve-shortening flow under which all n-gons asymptotically approach a regular n-gon?*

In Sections 4 and 5 we discuss two polygon flows in detail: the linear semidiscrete flow and the β-polygon flow. Notably, the β-polygon flow could be a flow that produces regular polygons. In Section 6 we compute several numerical examples which support this idea.

Other polygon flows in the literature include a scheme that approximates the continuous curve-shortening flow [14] and another that uses the Menger curvature, which is the curvature of the circle defined by three points [15].

4 Linear Semidiscrete Curve-Shortening

In this section we describe the semidiscrete curve-shortening flow of Chow and Glickenstein [2]. Some of the tools developed here become useful when working with the β-polygon flow in Section 5.

To develop a curve-shortening scheme on a polygon X we need a notion of a normal direction in which to evolve each vertex. We define the *polygonal normal* at vertex X_i as

$$N_i = (X_{j+1} - X_j) + (X_{j-1} - X_j),$$

where indices are taken mod n. This normal can be thought of as the the fourth vertex of the parallelogram defined by X_{i-1}, X_i and X_{i+1}, illustrated in Figure 5.

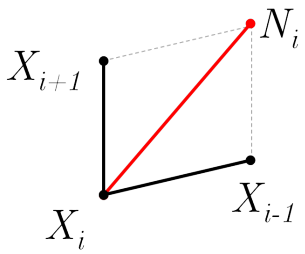

Figure 5: The polygonal normal N_i at the vertex X_i on a section of a polygon.

The semidiscrete flow simply evolves a polygon in the direction of the polygonal normal at each vertex.

Definition 4. *A polygon $X(t)$ satisfies the linear semidiscrete curve-shortening flow if for $j = 0, \ldots, n-1$,*

$$\frac{dX_j}{dt} = (X_{j+1} - X_j) + (X_{j-1} - X_j) = X_{j-1} - 2X_j + X_{j+1}, \tag{2}$$

where indices are taken mod n.

Since this flow is linear we can write it as the matrix equation

$$\frac{dX}{dt} = MX,$$

where

$$M = \begin{pmatrix} -2 & 1 & 0 & \cdots & 0 & 1 \\ 1 & -2 & 1 & 0 & \ddots & 0 \\ 0 & 1 & -2 & 1 & 0 & \vdots \\ \vdots & 0 & \ddots & \ddots & \ddots & 0 \\ 0 & \ddots & 0 & 1 & -2 & 1 \\ 1 & 0 & \cdots & 0 & 1 & -2 \end{pmatrix}. \tag{3}$$

The eigenvectors and eigenvalues of the matrix M are well-understood, which allows us to write an explicit solution for the flow. In Section 4.1 we describe properties of the matrix M and in Section 4.2 we state a result characterizing the long-term behavior of the flow.

4.1 Matrix Properties

The matrix M is a *circulant matrix*. Circulant matrices take the form

$$A = \begin{pmatrix} a_0 & a_1 & a_2 & \cdots & a_{n-2} & a_{n-1} \\ a_{n-1} & a_0 & a_1 & \cdots & a_{n-3} & a_{n-2} \\ \vdots & \vdots & \vdots & \vdots & \vdots & \vdots \\ a_2 & a_3 & a_4 & \ldots & a_0 & a_1 \\ a_1 & a_2 & a_3 & \ldots & a_{n-1} & a_0 \end{pmatrix}.$$

Circulant matrix theory allows us to write down the eigenvectors and eigenvalues of M. Let $\omega = e^{2\pi i/n}$. Integer powers of ω are known as *n^{th} roots of unity* since they are solutions of the equation $z^n = 1$. The matrix M has eigenvectors consisting of n^{th} roots of unity.

Proposition 4.1 (Chow and Glickenstein, 2007)**.** *The matrix M has eigenvectors*

$$P_k = (1, \omega^k, \omega^{2k}, \ldots, \omega^{(n-1)k})^T,$$

with corresponding eigenvalues

$$\lambda_k = -4\sin^2(k/2\pi)$$

for $k = 0, \ldots, n-1$.

If we plot each entry of an eigenvector of M in the complex plane and connect consecutive entries with arrows, the result is a regular polygon or pentagram. For this reason, the eigenvectors of M are also called *eigenpolygons*. Interestingly, some eigenpolygons have the same edges, but a different orientation. For example, in the $n = 3$ case, the eigenvectors $P_1 = (1, \omega, \omega^2)$ and $P_2 = (1, \omega^2, \omega^4 = \omega)$ represent the the same triangle but arrows are reversed. For any n-gon, the eigenvector $P_0 = (1, 1, \ldots, 1)^T$ is represented as the point $(1, 0)$ and so it is considered trivial. All non-trivial eigenpolygons with counterclockwise orientation for $n = 3, \ldots, 9$ are shown in Figure 6.

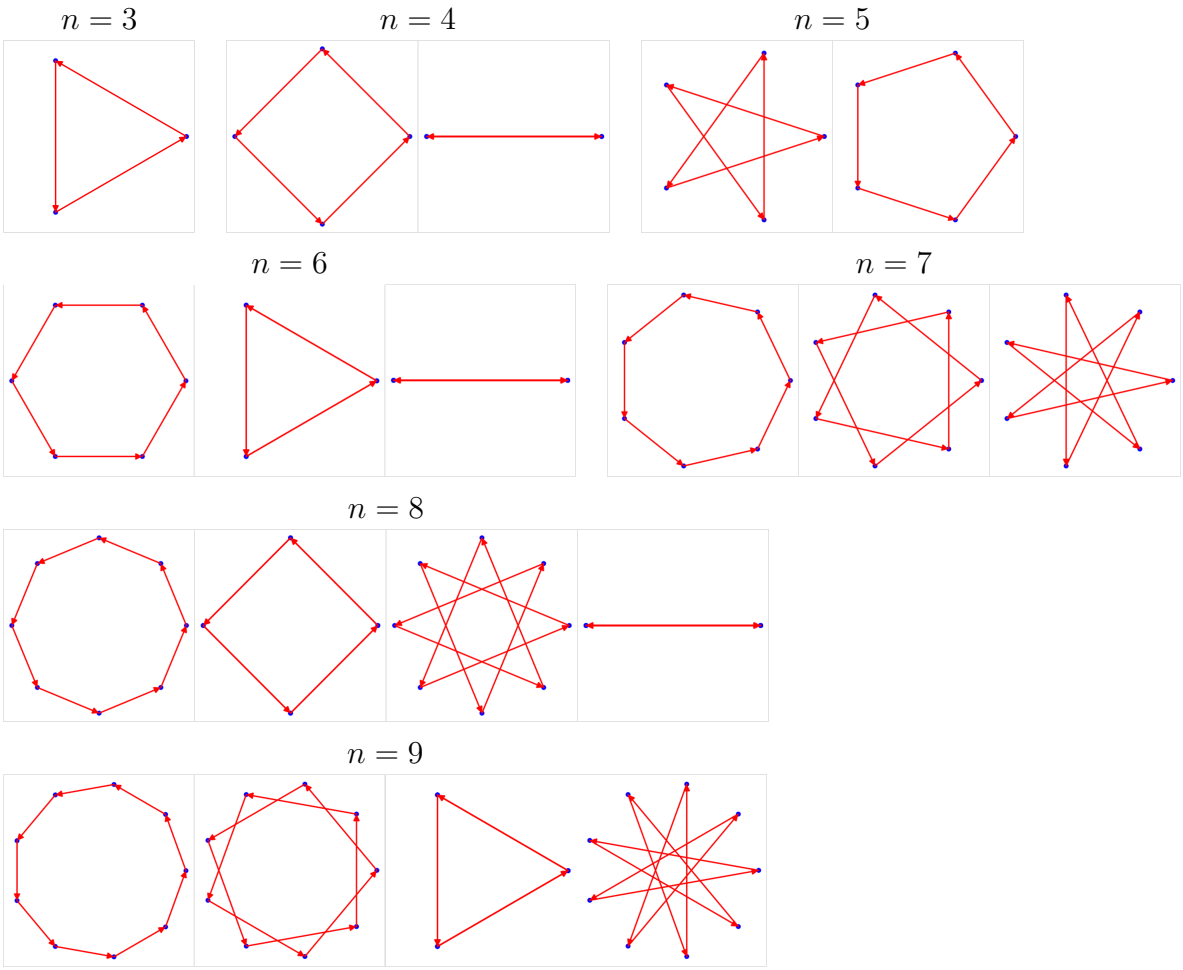

Figure 6: All non-trivial eigenpolygons up to orientation for $n = 3, \ldots, 9$.

Furthermore, the matrix M has rank n and so the eigenpolygons $P_0, \ldots, P_{n-1}$ form a basis for $\mathbb{C}^n$. Thus, any polygon X in $\mathbb{R}^2$ can be written as

$$X = c_0 P_0 + c_1 P_1 + \cdots + c_{n-1} P_{n-1}, \tag{4}$$

where $c_0, \ldots, c_{n-1}$ are complex weights. The map $X_i \to c_i$ is called the *discrete Fourier transformation* and is described in [2].

4.2 Long-Time Behavior

Using the weights $c_0, \ldots, c_{n-1}$ from (4), the solution to the linear semidiscrete flow (2) for a polygon X in $\mathbb{R}^2$ can be written as

$$X(t) = \sum_{i=0}^{n-1} c_i e^{\lambda_i t} P_i.$$

Using this solution, it can be shown that the flow produces affine transformations of regular polygons. In other words, if X asymptotically approaches Y under (2), there exists a rescaling of Y called Y', an $n \times n$ matrix B and a vector b such that

$$Y' = BP_1 + b.$$

This result is described in Theorem 4.1.

Theorem 4.1 (Chow and Glickenstein, 2007)**.** *Under the semidiscrete flow* (2) *in* $\mathbb{R}^2$*, every polygon with* n *vertices shrinks to a point. As it shrinks to a point, it converges asymptotically to an affine transformation of a convex regular* n*-gon, unless the initial polygon is orthogonal to the convex regular* n*-gon.*

An analogous result also holds for polygons in higher dimensions.

Theorem 4.2 (Chow and Glickenstein, 2007)**.** *Under the semidiscrete flow* (2) *in* $\mathbb{R}^p$*, every polygon with* n *vertices in* $\mathbb{R}^p$ *shrinks to a point and asymptotically becomes the linear image of a convex regular* n*-gon in* $\mathbb{R}^2$*.*

Importantly, the semidiscrete flow does not always produce regular polygons. In fact, as noticed in [3], all triangles and quadrilaterals are affinely regular, so the space of polygons produced by the flow is large. However, a generalization of the semidiscrete flow, called the β-polygon flow, may deform most polygons into regular polygons. This flow is discussed in Section 5.

5 The β-polygon Flow

The β-polygon flow, introduced by Glickenstein and Liang, generalizes the linear semidiscrete flow by scaling the components of the polygonal normal by edge lengths [3]. We only consider the actions of the flow on polygons in $\mathbb{R}^2$.

Definition 5. *Let* $\beta > 0$*. Consider all indices mod* n*. For* $j = 0, \ldots, n-1$*, define* $l_j = |X_{j+1} - X_j|$*. A polygon* X *in* $\mathbb{R}^2$ *satisfies the* β*-polygon flow if*

$$\frac{dX_j}{dt} = l_j^{\beta}(X_{j+1} - X_j) + l_{j-1}^{\beta}(X_{j-1} - X_j). \tag{5}$$

Notice that if we set $\beta = 0$, the β-polygon flow reduces to the linear semidiscrete flow (2).

The matrix form of the β-polygon flow is given by

$$\frac{dX}{dt} = M_X X,$$

where

$$M_X = \begin{pmatrix} -(l_0^\beta + l_{n-1}^\beta) & l_0^\beta & 0 & \cdots & 0 & l_{n-1}^\beta \\ l_0^\beta & -(l_0^\beta + l_1^\beta) & l_1^\beta & 0 & \ddots & 0 \\ 0 & l_1^\beta & -(l_1^\beta + l_2^\beta) & l_2^\beta & 0 & \vdots \\ \vdots & 0 & \ddots & \ddots & \ddots & 0 \\ 0 & \ddots & 0 & l_{n-3}^\beta & -(l_{n-3}^\beta + l_{n-2}^\beta) & l_{n-2}^\beta \\ l_{n-1}^\beta & 0 & \cdots & 0 & l_{n-2}^\beta & -(l_{n-2}^\beta + l_{n-1}^\beta) \end{pmatrix}.$$

The notation M_X is used for the matrix equation (rather than, say, just M) since the system of differential equations depends on the edge lengths $l_0, \ldots, l_{n-1}$ of the specific polygon X.

5.1 Derivation

A *functional* is a function from a vector space to its scalar field. The β-polygon flow is motivated by the gradient of the functional

$$F_\alpha(X) = \frac{1}{\alpha} \sum_{j=0}^{n-1} |X_{j+1} - X_j|^\alpha. \tag{6}$$

The negative gradient of the functional F is the vector

$$-\nabla F = \left\langle -\frac{\partial F}{\partial X_0}, -\frac{\partial F}{\partial X_1}, \ldots, -\frac{\partial F}{\partial X_0} \right\rangle.$$

We can compute the i^{th} component of $-\nabla F$ as

$$\begin{aligned} -\frac{\partial F}{\partial X_i} &= -\frac{1}{\alpha} \frac{\partial}{\partial X_i} \left[|X_i - X_{i-1}|^\alpha + |X_{i+1} - X_i|^\alpha \right] \\ &= -\frac{1}{\alpha} \frac{\partial}{\partial X_i} \left[\left(\sqrt{(X_i - X_{i-1})^2} \right)^\alpha + \left(\sqrt{(X_{i+1} - X_i)^2} \right)^\alpha \right] \\ &= -\frac{1}{\alpha} \left[\frac{\alpha(2X_i - 2X_{i-1})}{2|X_i - X_{i-1}|^{2-\alpha}} + \frac{\alpha(-2X_{i+1} + 2X_i)}{2|X_{i+1} - X_i|^{2-\alpha}} \right] \\ &= -\left[-\frac{(X_{i-1} - X_i)}{|X_i - X_{i-1}|^{2-\alpha}} - \frac{(X_{i+1} - X_i)}{|X_{i+1} - X_i|^{2-\alpha}} \right] \\ &= l_i^{\alpha-2}(X_{i+1} - X_i) + l_{i-1}^{\alpha-2}(X_{i-1} - X_i). \end{aligned} \tag{7}$$

Letting $\beta = \alpha - 2$, the flow (7) is precisely the β-polygon flow (5). We call this flow the *negative gradient flow* of the functional (6). Deriving a flow from a functional in this context makes it susceptible to tools from the calculus of variations.

5.2 Properties of the Flow

A *Euclidean isometry* is a distance persevering map in Euclidean space. In the plane, Euclidean isometries consist of translations, rotations and reflections. Proposition 5.1 states that the β-polygon flow is invariant under Euclidean isometries and scalar multiplication and that the center of mass of a polygon is preserved by the flow.

Proposition 5.1 (Glickenstein and Liang, 2016)**.** *Let X be a polygon, $c > 0$ and E by a Euclidean isometry of the plane. Denote the action of E on X by XE. Then,*

1. $M_{XE} = M_X$.
2. $M_{cX} = c^\beta M_X$.
3. *The center of mass, $\frac{1}{n}\sum_{i=0}^{n-1} X_i$, is preserved by the flow.*

Proof. The first follows from the fact that M_X only depends on edge lengths, not on vertices.

To establish the second, notice that multiplying each point in X by c has the effect of scaling the edge lengths of X by c and so we can factor c^β out of each entry in M_{cX} to write $M_{cX} = c^\beta M_X$.

Finally, notice that the row sums of M_X are 0. Hence, $\sum_{i=0}^{n-1} \frac{dX_i}{dt} = 0$ and so $\sum_{i=0}^{n-1} X_i(t)$ is constant for all time t. Therefore, the center of mass is preserved by the flow. □

5.3 Self-Similar Solutions

A self-similar solution to the β-polygon flow (5) has the same shape throughout the evolution up to shifting and scaling.

Definition 6. *We say $X(t)$ is self-similar solution of the β-polygon flow if there exists a polygon X_0, a scaling function $\lambda(t)$ and a point Q such that $\lambda(t)X_0 + Q$ satisfies* (5)*.*

The invariance properties in Proposition 5.1 help us establish that regular polygons are self-similar solutions to (5). Recall that P_k is the k^{th} eigenpolygon given in Proposition 4.1.

Theorem 5.1. *The regular n-gon P_k is a self-similar solution to the β-polygon flow* (5)*.*

Proof. Let $a(t)$ be a scaling function. As an ansatz, suppose $P(t) = a(t)P_k$ is a solution to the flow (5). Using the invariance properties,

$$\frac{dP}{dt} = \frac{da}{dt}P_k = M_P P = M_{aP_k}(aP_k) = a^{\beta+1}M_{P_k}P_k.$$

Since P_k is a regular polygon, all side lengths are equal, i.e. $l_0 = l_1 = \cdots = l_{n-1}$. Accordingly, let l be the side length of P_k. Then $M_{P_k} = l^\beta M$ where M is the matrix (3). It follows that

$$a^{\beta+1}M_{P_k}P_k = a^{\beta+1}l^\beta M P_k = a^{\beta+1}l^\beta \lambda_k P_k,$$

where λ_k is the eigenvalue of M corresponding to eigenvector P_k. By definition, $\frac{dP}{dt} = \frac{da}{dt}P$ and so

$$\frac{da}{dt} = a^{\beta+1}l^\beta\lambda_k.$$

This is a separable differential equation and so to solve we can integrate

$$\int a^{-\beta-1}da = \int l^\beta \lambda_k dt.$$

The general solution is $\frac{-1}{\beta}a^{-\beta} = l^\beta\lambda_k t + C$. With $a(0) = 1$, we find $a(t) = (1 - \beta l^\beta\lambda_k t)^{-1/\beta}$. Therefore, since there exists a function $a(t)$ such that $P(t) = a(t)P_k$ is a solution to (5), the regular polygon P_k is a self-similar solution to the β-polygon flow. □

It follows from Theorem 5.1 that at any point during the flow a regular polygon will always look like a regular polygon before it shrinks to a point, illustrated in Figure 7.

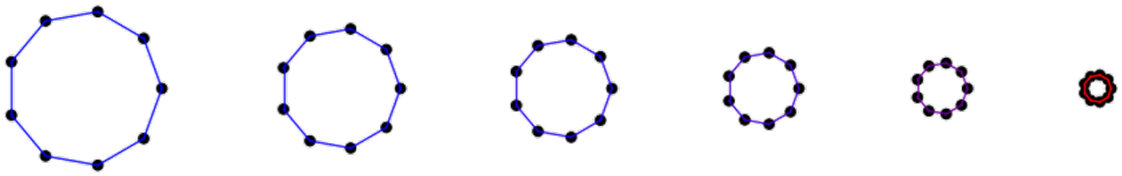

Figure 7: A regular nonagon shrinks self-similarly under the β-polygon flow.

5.4 Stability Results

Our goal is to characterize the shapes of polygons that are approached asymptotically under the β-polygon flow. These "limit polygons" have not been fully-characterized, but some stability results exist. In the case of the triangle, all limit polygons are regular.

Theorem 5.2 (Glickenstein and Liang, 2016)**.** *Under the β-polygon flow, an arbitrary (non-degenerate) triangle shrinks to a point and converges to a regular triangle if appropriately rescaled.*

For $n \geq 5$, polygons close in shape to a regular n-gon converge to a regular n-gon.

Theorem 5.3 (Glickenstein and Liang, 2016)**.** *Assume $n \geq 5$. Under the β-polygon flow, any regular n-gon shrinks to a point and is asymptotically stable in the sense that there is a neighborhood such that the polygons in that neighborhood converge to a regular polygon under the β-polygon flow if appropriately re-scaled.*

A weaker result holds for $n = 4$.

Theorem 5.4 (Glickenstein and Liang, 2016)**.** *When $n = 4$, the shape of square is locally stable on a 7-dimensional hypersurface under the β-polygon flow.*

5.5 Rescaled Flow

In order to investigate the long-term behavior of the β-polygon flow on different polygons we consider a rescaled version of the flow in which the regular polygon P_1 is a fixed point. In other words, the evolution equation for the rescaled flow is zero when the polygon is P_1. Instead of shrinking to a point, polygons are rescaled as they are deformed by this flow and so we can observe their shape as they evolve.

To formulate this rescaled flow we shift and scale a solution to the original flow. Let X be a solution to the β-polygon flow (5), let $\alpha : \mathbb{R} \to \mathbb{R}^+$ be a positive scaling function and let $\bar{X}$ denote the n-vector in which each entry is the center of mass of X. Consider the polygon $Y := \alpha(X - \bar{X})$. Multiplying by α rescales the solution and subtracting $\bar{X}$ shifts X so its center of mass is at the origin (see Figure 8).

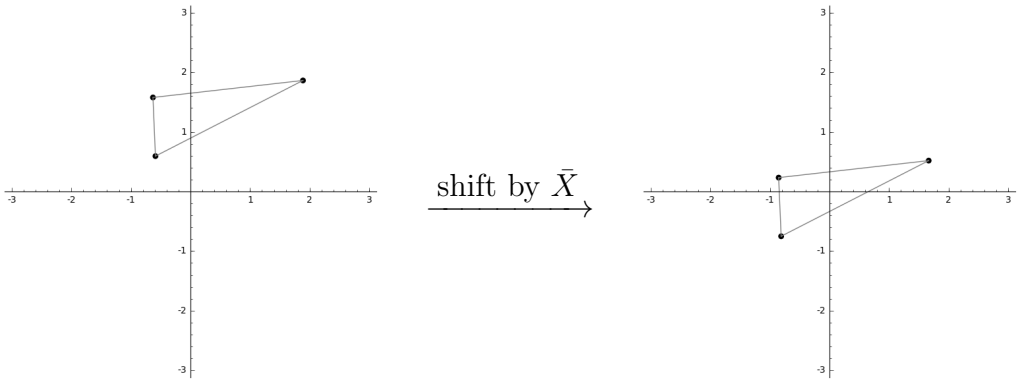

Figure 8: Shifting a polygon so its center of mass is at the origin.

Using the invariance properties in Proposition 5.1, the evolution of Y is given by

$$\begin{aligned}\frac{dY}{dt} &= \frac{d}{dt}(\alpha(X-\bar{X})) \\ &= \frac{d\alpha}{dt}(X-\bar{X}) + \alpha M_X X \\ &= \frac{d\alpha}{dt}\frac{1}{\alpha}(\alpha(X-\bar{X})) + \frac{1}{\alpha^\beta} M_{\alpha(X-\bar{X})} \\ &= \frac{d\alpha}{dt}\frac{1}{\alpha} Y + \frac{1}{\alpha^\beta} M_Y Y.\end{aligned}$$

We would like P_1 to be a fixed point of the rescaled flow. Accordingly, let $\alpha(t) = 1/a(t)$, where $a(t) = (1-\beta l^\beta \lambda_k t)^{-1/\beta}$ is the scaling function found in the proof of Theorem 5.1. Using $\frac{da}{dt} = a^{\beta+1} l^\beta \lambda_k$, we have

$$\frac{dY}{dt} = \frac{d\alpha}{dt}\frac{1}{\alpha} Y + \frac{1}{\alpha^\beta} M_Y Y = \left(\frac{-a'}{a^2}\right) aY + a^\beta M_Y Y = -a^\beta l^\beta \lambda_k Y + a^\beta M_Y Y.$$

To see that P_1 is a fixed point of this flow note that

$$-a^\beta l^\beta \lambda_k P_1 + a^\beta M_{P_1} P_1 = -a^\beta l^\beta M P_1 + a^\beta l^\beta M P_1 = 0.$$

In order to observe quicker convergence and remove dependence on $a(t)$, we adopt a new time variable. Define τ by $\frac{dt}{d\tau} = \frac{1}{l^\beta a^\beta}$. Then,

$$\begin{aligned}\frac{dY}{d\tau} &= \frac{dY}{dt}\frac{dt}{d\tau} \\ &= (-a^\beta l^\beta \lambda_k Y + a^\beta M_Y Y)\left(\frac{1}{l^\beta a^\beta}\right) \\ &= -\lambda_1 Y + \frac{1}{l^\beta} M_Y Y.\end{aligned}$$

We define the *rescaled β-polygon flow* by the evolution equation

$$\frac{dY}{d\tau} = -\lambda_1 Y + \frac{1}{l^\beta} M_Y Y. \tag{8}$$

This new flow allows us to more easily observe the shapes of polygon while they evolve since a solution to this flow can be shifted and scaled to generate a solution to the original flow and vice versa. We use this flow to numerically compute the trajectories of different polygons in Section 6.

6 Numerical Solutions

In this section we numerically solve the rescaled β-polygon flow (8) to investigate the asymptotic shapes of different polygons under the flow. Our numerical evidence suggests that polygons with more than 5 vertices approach a regular polygon and quadrilaterals become rhombic.

In Section 6.1 we outline the numerical method we used to approximate the trajectories of polygons under the rescaled flow and in Sections 6.2-6.4 we discuss several examples. All figures were created in `Sage`.

6.1 Approximation Technique

Since we do not have an explicit solution to the evolution equation for the rescaled β-polygon flow (8), we approximate the solution using numerical methods. Specifically we use *Euler's Method*, a local linearization algorithm that approximates solutions to differential equations, to generate discrete approximations of the trajectories of polygons under the flow.

Let Y be a polygon. To better understand the approximation we identify the vertices of Y with points in $\mathbb{R}^2$, writing

$$Y = \begin{pmatrix} Y_0 \\ Y_1 \\ \vdots \\ Y_{n-1} \end{pmatrix} = \begin{pmatrix} (x_0,\ y_0) \\ (x_1,\ y_1) \\ \vdots \\ (x_{n-1},\ y_{n-1}) \end{pmatrix}.$$

The polygon Y is used as our initial condition. Let $x_j^{(i)}$ and $y_j^{(i)}$ denote the values of x_j and y_j respectively at time $\tau = i$.

Let $f := \frac{dY_j}{d\tau}$. Since f depends on the vertices Y_{j-1}, Y_j and Y_{j+1} and outputs a vertex, it is a function from $\mathbb{R}^6$ to $\mathbb{R}^2$. Write $f = (f_x, f_y)$. Using the rescaled β-polygon flow (8),

$$f_x = -\lambda_1 x_j^{(i)} + \frac{1}{l^\beta}\left(l_j^\beta (x_{j+1}^{(i)} - x_j^{(i)}) + l_{j-1}^\beta (x_{j-1}^{(i)} - x_j^{(i)})\right).$$

The y-component of f is analogous.

Treating Y as the initial condition, the approximation is defined by the equations

$$\begin{aligned} x_j^{(i+1)} &= x_j^{(i)} + hf(x_{j-1}^{(i)},\ y_{j-1}^{(i)},\ x_j^{(i)},\ y_j^{(i)},\ x_{j+1}^{(i)},\ y_{j+1}^{(i)}), \\ y_j^{(i+1)} &= y_j^{(i)} + hf(x_{j-1}^{(i)},\ y_{j-1}^{(i)},\ x_j^{(i)},\ y_j^{(i)},\ x_{j+1}^{(i)},\ y_{j+1}^{(i)}). \end{aligned}$$

The parameter h is known as the *step size* and is the distance between successive time steps during the approximation. If we iterate this process N times then the trajectory of the vertex Y_j is given by

$$\mathcal{T}_j = \{(x_j^i, y_j^i) \mid i = 0, \ldots, N\}.$$

To approximate the evolution for $0 \leq \tau \leq T$ we compute $N = T/h$ time-steps.

In Sections 6.2-6.4, we use this scheme with a step size of $h = 0.01$ to approximate the trajectories of different polygons under the β-polygon flow.

6.2 A Triangle

Theorem 5.2 states that every triangle asymptotically approaches a regular triangle under the β-polygon flow. This is illustrated by the evolution of a triangle in Figure 9.[1]

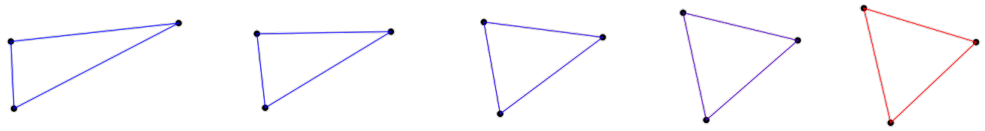

Figure 9: Selected frames from the evolution of a triangle under the rescaled β-polygon, with $\beta = 1$ for $0 \leq \tau \leq 5$.

The angles and side lengths of the triangle during the evolution process are shown in Figure 10.

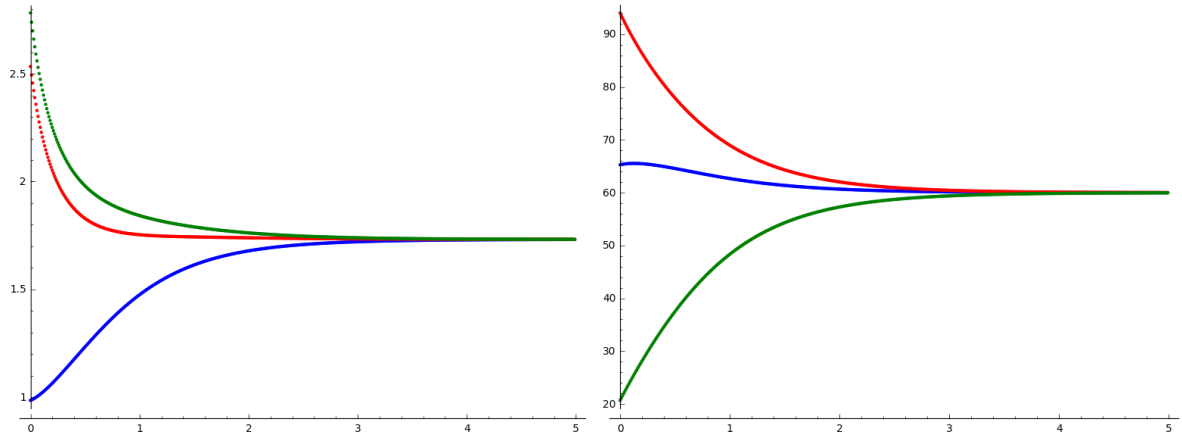

(a) Side lengths l_0, l_1, l_2 over time τ (b) Angles $\theta_0, \theta_1, \theta_2$ over time τ

Figure 10: The evolution of sides and angles of a triangle under the rescaled β-polygon flow.

Notice that the angles of the triangle are each approaching 60° and side lengths are approaching a fixed value. This example demonstrates how triangles become regular under the flow.

[1] Animations of Figures 9, 11, 13a and 14a are available at `youtu.be/dBh63BNxW5E`.

6.3 A Quadrilateral

Unlike the triangle, Theorem 5.4 only provides a week stability result for the square. Furthermore, as first noticed in [3, Figure 4], quadrilaterals do seem to become square under the rescaled β-polygon flow. This is demonstrated by the example in Figure 11.

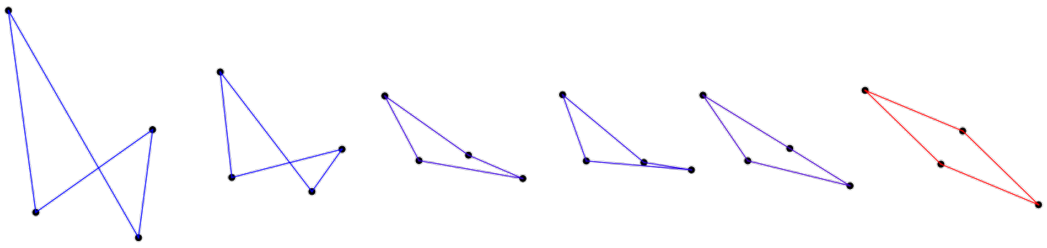

Figure 11: Selected frames from the evolution of a quadrilateral under the β-polygon, with $\beta = 1$ for $0 \leq \tau \leq 5$.

Since this quadrilateral does not approach a square shape its limit polygon is not equiangular. However, the quadrilateral appears to approach a rhombus, an equilateral polygon. This idea is supported by the evolution of the side lengths and angles shown in Figure 12.

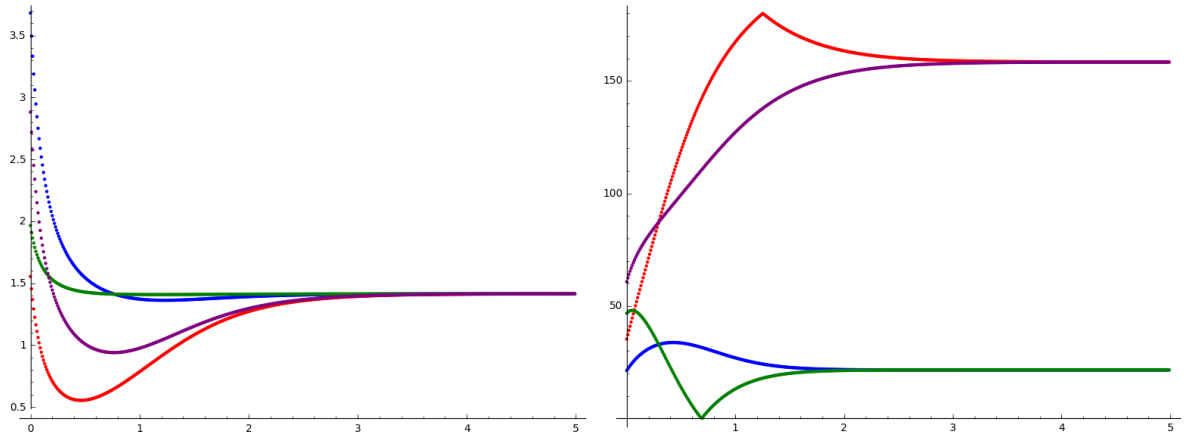

(a) Side lengths (b) Angles

Figure 12: The evolution of sides and angles of a quadrilateral under the rescaled β-polygon flow.

Notice that all four side lengths are approaching a fixed value and opposite angles are approaching fixed values. Other examples of quadrilaterals we considered exhibit the same behavior and so we conjecture that all quadrilaterals become rhombic under the rescaled β-polygon flow. We also observed that applying if we apply small perturbations to the square, the limiting shape of the resulting polygon is not equiangular but it is equilateral. This indicates that the square itself may be the only polygon that becomes asymptotically square under the flow.

6.4 Larger n-gons

In the case of $n \geq 5$, to show that a polygon is becoming regular it suffices to show that it is asymptotically becoming equilateral or equiangular, since these are equivalent conditions. Figures 13 and 14 show examples of polygons in the $n = 5$ and $n = 6$ cases in which angles and side lengths approach fixed points. This indicates that they are becoming regular. We conjecture that for $n \geq 5$, all polygons become regular under the rescaled β-polygon flow.

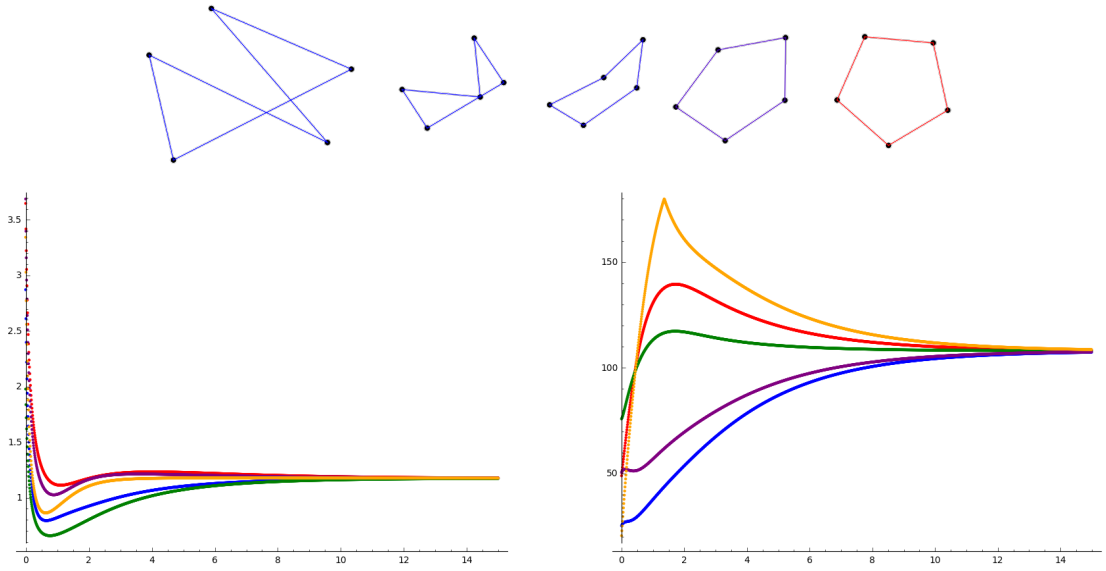

(a) Side lengths (b) Angles

Figure 13: The evolution of a pentagon under the rescaled β-polygon flow.

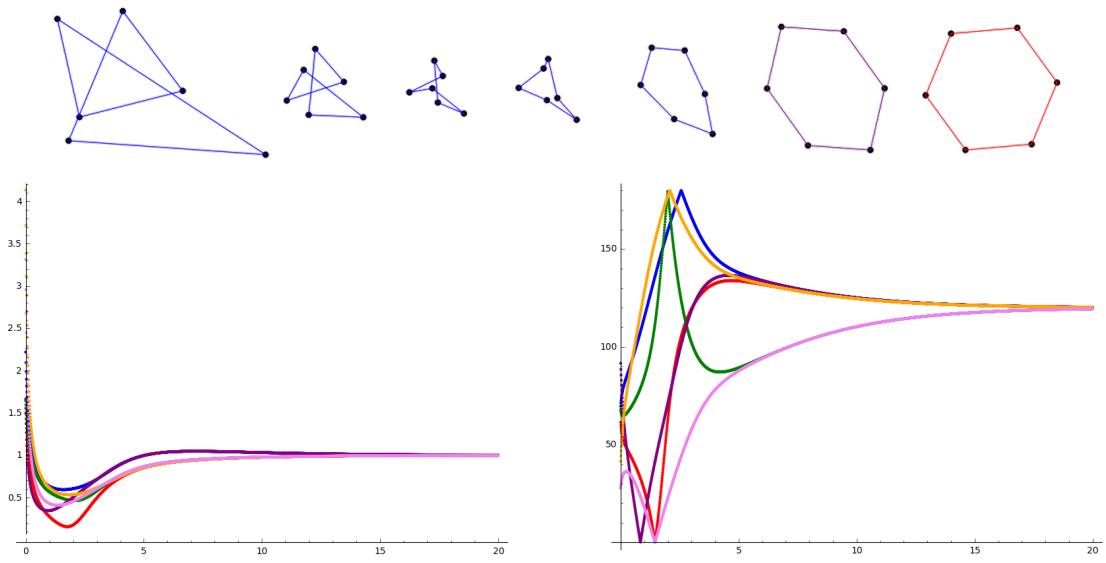

(a) Side lengths (b) Angles

Figure 14: The evolution of a hexagon under the rescaled β-polygon flow.

7 Discussion

Semidiscrete curve-shortening flows are meant to approximate the behavior of the continuous curve-shortening flow. However, no flow has been identified that asymptotically deforms polygons into regular polygons.

The linear semidiscrete flow described in Section 4 is currently the only semidiscrete scheme for which we have an explicit solution. Other flows, such as the β-polygon flow, are nonlinear and so finding an explicit solution is difficult. Hence, numerical methods are a useful tool to look at at the trajectories of polygons under semidiscrete flows. Our results lead us to conjecture that a quadrilateral converges to a rhombus and for $n \geq 5$, an n-gon converges to a regular n-gon. Our numerical evidence could be used to inform future theoretical results about the β-polygon flow.

Furthermore, with the numerical framework in place, our approximation methods could be extended to investigate the trajectories of other polygon flows such as those in [14, 15]. Techniques in numerical analysis could be applied to fit the trajectories of points to known curves to classify how fast different polygons converge. The intuition generated by numerical insights could someday be helpful in establishing theoretical stability results about polygon flows. Notably, proving that some semidiscrete flow asymptotically deforms polygons into regular polygons would be an important contribution.

Acknowledgments. This paper is part of the author's Senior Seminar project in partial fulfillment of the Mathematics major at Ripon College. The author thanks project mentor Dr. Andrea Young for her guidance.

References

[1] Sigurd Angenent. Curve shortening makes a plane curve convex. YouTube, https://youtu.be/wHfpacPLHIA., 2011.

[2] Bennett Chow and David Glickenstein. Semidiscrete geometric flows of polygons. *The American Mathematical Monthly*, 114(4):316–328, 2007.

[3] David Glickenstein and Jinjin Liang. Asymptotic behavior of β-polygon flows. arXiv:1610.03598, 2016.

[4] John Oprea. *Differential Geometry and Its Applications: Second Edition*. 2004.

[5] Connor Mooney. An introduction to curve-shortening and the ricci flow, 2011.

[6] M. Gage and R. S. Hamilton. The heat equation shrinks convex plane curves. *Journal of Differential Geometry*, 23:69–96, 1986.

[7] M. Grayson. Shortening embedded curves. *Annals of Mathematics*, 129:71–111, 1989.

[8] Yun Yan Yang and Xiao Xiang Jiao. Curve shortening flow in arbitrary dimensional euclidian space. *Acta Mathematica Sinica*, 21(4):715–722, 2005.

[9] Hoeskuldur P. Halldorsson. Self-similar solutions to the curve shortening flow. 2010.

[10] Manuel Ritor and Carlo Sinestrari. *Mean Curvature Flow and Isoperimetric Inequalities (Advanced Courses in Mathematics - CRM Barcelona)*. Birkhuser, 2010.

[11] S. L. Smith, M. E. Broucke, and B. A. Francis. Curve shortening and the rendezvous problem for mobile autonomous robots. *IEEE Transactions on Automatic Control*, 52, 2007.

[12] A. Tannenbaum. Three snippets of curve evolution theory in computer vision. *Mathematical and Computer Modelling*, 24(5):103 – 119, 1996.

[13] Alfred M. Bruckstein, Guillermo Sapiro, and Doron Shaked. Evolutions of planar polygons. *International Journal of Pattern Recognition and Artificial Intelligence*, 9(06):991–1014, 1995.

[14] K. Nakayama, H. Segur, and M. Wadati. A discrete curve-shortening equation. *Methods and Applications of Analysis*, 4:162–172, 1997.

[15] Thierry Jecko and Jean-Christophe Léger. Polygon shortening makes (most) quadrilaterals circular. *Bulletin of the Korean Mathematical Society*, 39(1):97–111, 2002.